MR-MCTDH[n]: Flexible configuration spaces and non-adiabatic dynamics within the MCTDH[n] framework

Niels Kristian Madsen,*,† Mads Bøttger Hansen,† Graham A. Worth,‡ and Ove Christiansen†

†*Department of Chemistry, University of Aarhus, Langelandsgade 140, DK–8000 Aarhus C, Denmark*

‡*Department of Chemistry, University College London, 20, Gordon St. WC1H 0AJ London, United Kingdom*

E-mail: nielskm@chem.au.dk

Abstract

Solving the time-dependent Schrödinger equation (TDSE) for large molecular systems is a complicated task due to the inherent exponential scaling of the problem. One of the most successful and versatile methods for obtaining numerically converged solutions for small to medium-sized systems is multiconfiguration time-dependent Hartree (MCTDH). In a recent publication [J. Chem. Phys. **152**, 084101 (2020)] we introduced a hierarchy of approximations to the MCTDH method which mitigate the exponential scaling by truncating the configuration space based on a maximum excitation level w.r.t. a selected reference configuration. The MCTDH[n] methods are able to treat large systems, but the single-reference Ansatz is not optimal in cases where one (or a few) degrees of freedom are special. Examples could be double-well systems, intramolecular vibrational-energy redistribution (IVR) calculations, or non-adiabatic dy-

namics. In this work we introduce a multi-reference (MR) extension to the MCTDH[n] methods where selected higher-order excitations for the special degrees of freedom can be introduced in a simple but flexible way. The resulting MR-MCTDH[n] methods allow for e.g. treating non-adiabatic dynamics within the single-set formalism with the wave packets on each electronic surface described using the same level of approximation. Example calculations are performed on formyl fluoride (IVR), salicylaldimine (double well), and pyrazine (non-adiabatic dynamics). The results show that fast convergence is achieved by extending the configuration space in the special modes that govern the quantum dynamics.

1 Introduction

The ability to simulate the quantum dynamics of complex molecular systems is of great importance in chemical physics. Quantum-mechanical calculations are valuable tools for e.g. interpreting photoabsorption spectra, reaction rates, and for studying the behavior of molecules exposed to time-dependent perturbations. Solving the time-dependent Schrödinger equation (TDSE) exactly is, however, impossible for anything but the smallest systems due to the inherent exponential scaling w.r.t. system size known as the *curse of dimensionality*. One of the most sucessful methods for obtaining numerically converged solutions to the TDSE for molecules with more than ~ 4 atoms is multiconfiguration time-dependent Hartree (MCTDH)[1,2]. The MCTDH method still scales exponentially with system size, but the base is reduced significantly by expanding the wave packet in a compact time-dependent basis which adapts itself variationally to the time evolution of the wave function. MCTDH includes the exact method as a limiting case and if the number of time-dependent basis functions (denoted as time-dependent modals or single-particle functions (SPFs)) is set to one for all degrees of freedom, MCTDH reduces to time-dependent Hartree (TDH)[2–4]. The TDH method provides a mean-field description of the correlation between modes by representing the wave packet as a single Hartree product. It thus reduces the computational scaling

significantly which allows application of TDH to very large systems[3]. However, for many systems of interest a correlated wave-function description is required for obtaining even qualitatively correct results[4].

Over the years many extensions and alternatives to MCTDH have been formulated with the aim of reducing computational cost or increasing computational flexibility in various ways. Among these are multilayer MCTDH (ML-MCTDH)[5–8] and various methods based on variational Gaussian wave packets, such as G-MCTDH[9,10] and variational multi-configurational Gaussian (vMCG)[11,12], which are in turn related to the coupled coherent states (CCS)[13,14] and multiple-spawning[15–17] methods. The MCTDH[n] method presented in Ref. 18 reduces the computational scaling of MCTDH by truncating the number of configurations based on excitation level w.r.t. a reference configuration in line with the vibrational configuration interaction (VCI)[19,20] and vibrational coupled cluster (VCC)[21–23] methods for solving the time-independent Schrödinger equation (TISE), and also very recently time-dependent vibrational coupled cluster (TDVCC) theory.[24] Schemes for the truncation of the configuration space in MCTDH have been developed in previous works[25–28] and outside the MCTDH context the topic has been studied extensively for both time-dependent[29–32] and time-*in*dependent[21,33–38] wave functions. While the previous works on truncated MCTDH have primarily focused on obtaining a fully converged wave-function description, the aim of MCTDH[n] is to introduce a systematic hierarchy of methods which allows a fully variational solution to the TDSE at each level of approximation to be obtained.

For a truncated MCTDH wave function to satisfy the time-dependent variational principle (TDVP), the so-called constraint (or gauge) operators g^m need to be chosen correctly (as also discussed in Ref. 25 and previous works on truncated MCTDH for systems of identical particles[39–42]). In the limit of full MCTDH the g^m operators can be chosen as arbitrary Hermitian one-mode operators, but if any configurations are removed from the wave function this is no longer the case. Previous works have employed a natural-orbital representation[2,43] of the wave function in the hope of keeping the weights of the missing configurations small.

The systematic nature of the MCTDH[n] truncation scheme allows an explicit analysis of the matrix elements of the g^m operators that become non-redundant and for writing a set of linear equations that determine the variationally optimal choice resulting in the MCTDH[n,V] methods. Alternatively, the constraint operators can be used to keep the one-mode density matrices block diagonal during the propagation resulting in the MCTDH[n,D] hierarchy. Setting $g^m = 0$ for all modes which is a standard choice in full MCTDH is denoted as MCTDH[n,g0]. Since different choices of g^m give different results, it is part of defining the method. It is therefore relevant to be explicit on this choice in computations, and from here on we avoid the word gauge since it is often associated with a freedom or invariance.

The MCTDH[n] expansion of the wave function is based on a single reference state. This provides an accurate description for many applications - especially when the constraint operators are chosen correctly[18]. However, when some degrees of freedom in the system are special, the wave function may attain multi-reference (MR) character. In those cases, selected higher-order excitations including the special modes are required for obtaining an accurate and balanced wave-function description. Examples of these systems could be double wells and non-adiabatic dynamics on coupled electronic states[44]. Schemes for constructing configuration spaces that allow special treatment of selected modes have previously been developed for computing vibrational energy levels with MCTDH in Refs. 26,27. In this work we introduce a flexible, yet simple, way of extending the configuration space of the MCTDH[n] methods in order to account for MR character in the selected modes. The resulting MR-MCTDH[n] methods include higher-order excitations for the special modes, and thus improve the description of the degrees of freedom that govern the dynamics of the system. This can be viewed as a special case of a more general framework for building the configuration space by assigning individual excitation weights to the modes. Note, that while both MCTDH and MCTDH[n] by name are multi-configurational methods, the multi-reference part of MR-MCTDH[n] refers to the specific way of selecting the configurational space. Both MCTDH[n] and MR-MCTDH[n] converge to full MCTDH, but the MR frame-

work provides a freedom for doing so in a more computationally efficient way when some degrees of freedom are special.

The remainder of the paper is structured as follows. Section 2 describes the MCTDH[n] approximation and introduces the equations of motion (EOMs) used for propagating the wave function. In section 3 the MR-MCTDH[n] extension is discussed and the implementation is described in section 4. Section 5 presents the numerical results while section 6 contains a summary and future outlook.

2 MCTDH[n] theory and extension to non-adiabatic dynamics

2.1 Summary of MCTDH theory in second quantization

For a system with M degrees of freedom (modes), the MCTDH wave function is written in second quantization (SQ) using the SQ formulation introduced in Ref. 19 and discussed for time-dependent wave functions in Refs. 3,18,24,

$$|\bar{\Psi}\rangle = \sum_{u^1=1}^{n^1} \cdots \sum_{u^M=1}^{n^M} C_{u^1 \ldots u^M}(t) \prod_{m=1}^{M} \tilde{a}^{m\,\dagger}_{u^m}(t)\,|\mathrm{vac}\rangle = \sum_{\mathbf{u}} C_{\mathbf{u}}\,|\tilde{\Phi}_{\mathbf{u}}\rangle \ , \tag{1}$$

where $|\tilde{\Phi}_{\mathbf{u}}\rangle$ is a Hartree product of time-dependent, one-dimensional functions denoted as single-particle functions or *modals*. The time-dependent modals are represented by a set of creation ($\tilde{a}^{m\,\dagger}_{u^m}$) and annihilation ($\tilde{a}^{m}_{u^m}$) operators which add and remove occupation in modal u^m of mode m, respectively. These elementary operators satisfy the commutator relations,

$$[\tilde{a}^{m}_{r^m}, \tilde{a}^{m'\,\dagger}_{s^{m'}}] = \delta_{mm'}\delta_{r^m s^{m'}} \tag{2a}$$

$$[\tilde{a}^{m}_{r^m}, \tilde{a}^{m'}_{s^{m'}}] = 0 \tag{2b}$$

$$[\tilde{a}^{m\,\dagger}_{r^m}, \tilde{a}^{m'\,\dagger}_{s^{m'}}] = 0 \ . \tag{2c}$$

SQ formulations are most commonly associated with systems of identical particles where the fundamental (anti-)commutator relations enforce the correct permutational symmetry. Such systems have been treated successfully with different variants of MCTDH[45–49]. As vibrational modes are distinguishable, permutational symmetry is not an issue in quantum molecular dynamics. The SQ formulation of MCTDH, however, leads to a short derivation of the EOMs[18] and key quantities (density matrices, mean fields, etc.) emerge naturally and resemble the analogues from e.g. electronic-structure theory (see table 1).

The time-dependent modals are expanded in a time-independent basis of size $N^m \geq n^m$ for each mode m. The use of a compact, time-dependent basis that adapts itself to the evolving wave packet is the primary strength of MCTDH which allows application of the method to much larger systems than the exact method[2]. However, the complete-active-space (or full-configuration-interaction) expansion makes the MCTDH method scale exponentially with M, limiting its applicability to small and medium-sized molecules.

Inserting Eq. (1) into the Dirac-Frenkel TDVP results in EOMs for the configuration-space coefficients and the time-dependent modals[18],

$$i\dot{C}_{\mathbf{u}} = \langle \tilde{\Phi}_{\mathbf{u}} | (H - g) | \bar{\Psi} \rangle \ , \tag{3}$$

$$i\dot{U}^m_{\alpha^m u^m} = \sum_{\beta^m} \left(\delta_{\alpha^m \beta^m} - \tilde{P}^m_{\alpha^m \beta^m} \right) \sum_{v^m} [(\tilde{\mathbf{D}}^m)^{-1}]_{u^m v^m} \check{F}^m_{v^m \beta^m} + \sum_{v^m} U^m_{\alpha^m v^m} \tilde{g}^m_{v^m u^m} \ , \tag{4}$$

where a linear parameterization has been chosen for the modals, i.e. for a general modal of mode m, indexed with r^m, we have $\tilde{a}^{m\,\dagger}_{r^m}(t) = \sum_{\alpha^m} a^{m\,\dagger}_{\alpha^m} U^m_{\alpha^m r^m}(t)$ and $\tilde{a}^m_{s^m}(t) = \sum_{\beta^m} a^m_{\beta^m} U^{m\,*}_{\beta^m s^m}(t)$, where $a^{m\,\dagger}_{\alpha^m}$ ($a^m_{\alpha^m}$) create (annihilate) occupation in the α^m'th time-independent basis function in mode m. Definitions of the various quantities appearing in Eqs. (3) and (4) are found in table 1.

Table 1: Definitions used in the MCTDH EOMs, Eqs. (3) and (4). See Ref. 18 for derivations and discussion of index conventions.

Constraint operators	$g = \sum_m g^m$	(5)
	$g^m = \sum_{u^m v^m} \tilde{g}^m_{u^m v^m} \tilde{a}^{m\dagger}_{u^m} \tilde{a}^m_{v^m}$	(6)
	$\tilde{g}^m_{u^m v^m} = i[\tilde{a}^m_{u^m}, \dot{\tilde{a}}^{m\dagger}_{v^m}]$	(7)
Density matrices	$\tilde{D}^m_{u^m v^m} = \langle \bar{\Psi} \vert \tilde{a}^{m\dagger}_{u^m} \tilde{a}^m_{v^m} \vert \bar{\Psi} \rangle$	(8)
Mean-field matrix elements	$\tilde{F}^m_{u^m r^m} = \langle \bar{\Psi} \vert \tilde{a}^{m\dagger}_{u^m} [\tilde{a}^m_{r^m}, H] \vert \bar{\Psi} \rangle$	(9)
	$\check{F}^m_{u^m \alpha^m} = \sum_{s^m} \tilde{F}^m_{u^m s^m} U^m_{\alpha^m s^m}$	(10)
Active-space projectors	$\tilde{P}^m_{\alpha^m \beta^m} = \sum_{u^m v^m} U^m_{\alpha^m u^m} [(\tilde{\mathbf{S}}^m)^{-1}]_{u^m v^m} U^{m*}_{\beta^m v^m}$	(11)
	$\tilde{S}^m_{u^m v^m} = [\tilde{a}^m_{u^m}, \tilde{a}^{m\dagger}_{v^m}]$	(12)

2.2 The MCTDH[n] approximation

The MCTDH[n] wave function is based on a single-reference Ansatz[18],

$$\vert \bar{\Psi} \rangle = C_{\mathbf{i}} \vert \tilde{\Phi}_{\mathbf{i}} \rangle + \sum_{\mathbf{m} \in \mathrm{MCR}[I]} \sum_{\mathbf{a^m}} C^{\mathbf{m}}_{\mathbf{a^m}} \vert \tilde{\mathbf{a}}^{\mathbf{m}} \rangle \ , \tag{13}$$

where $\vert \tilde{\Phi}_{\mathbf{i}} \rangle$ is the reference configuration. $\vert \tilde{\mathbf{a}}^{\mathbf{m}} \rangle \equiv \prod_{m \in \mathbf{m}} \tilde{a}^{m\dagger}_{a^m} \tilde{a}^m_{i^m} \vert \tilde{\Phi}_{\mathbf{i}} \rangle$ is a configuration where the reference (*occupied*) modals of the modes included in the mode combination (MC) $\mathbf{m}$ are excited to the *virtual* modals indexed by $a^m \ \forall \ m \in \mathbf{m}$. The wave function includes all excitations for all MCs in the mode-combination range (MCR) of included configurations denoted as MCR[I], i.e. the truncation is done solely in the sum over MCs and *not* in the $\mathbf{a^m}$ summation. The standard MCTDH[n] wave function includes all MCs of size $\leq n$, i.e. up to n-mode excitations w.r.t. the reference configuration. However, in principle any set

of MCs can be included in MCR[I] (the set must be closed under one-mode deexcitation in order to obtain a fully variational wave function[18]). This is used in section 3 for introducing the MR extension to the MCTDH[n] approximation.

An important aspect of the MCTDH[n] methods is the choice of constraint operators g^m. In the limit of $n = M$, i.e. full MCTDH, the g^m operators can be chosen to be arbitrary Hermitian one-mode operators and are often simply set to zero. Taking this approach in truncated MCTDH[n] results in the MCTDH[n,g0] methods. As shown in Ref. 18 this choice of constraint is, however, not optimal for achieving accurate results at low excitation levels because it does not satisfy the TDVP.

The non-redundant matrix elements of the constraint operators for the fully variational MCTDH[n,V] methods are obtained by solving a set of linear equations,

$$\sum_{m'} \sum_{b^{m'}} \mathcal{A}^{m\,m'}_{a^m b^{m'}} \tilde{g}^{m'}_{b^{m'} i^{m'}} = \mathcal{B}^{m}_{a^m} \ , \tag{14}$$

with,

$$\mathcal{A}^{m\,m'}_{b^m b^{m'}} \equiv \sum_{\mathbf{m}' \in \mathrm{MCR}[X_1] \,|\, m,m' \in \mathbf{m}'} \sum_{\mathbf{b}^{\mathbf{m}'}}^{-m,m'} C^{\mathbf{m}'\backslash m\ *}_{\mathbf{b}^{\mathbf{m}'\backslash m}} C^{\mathbf{m}'\backslash m'}_{\mathbf{b}^{\mathbf{m}'\backslash m'}} \ , \tag{15}$$

$$\mathcal{B}^{m}_{b^m} \equiv \sum_{\mathbf{m}' \in \mathrm{MCR}[X_1] \,|\, m \in \mathbf{m}'} \sum_{\mathbf{b}^{\mathbf{m}'}}^{-m} C^{\mathbf{m}'\backslash m\ *}_{\mathbf{b}^{\mathbf{m}'\backslash m}} \mathcal{K}^{\mathbf{m}'}_{\mathbf{b}^{\mathbf{m}'}} \ . \tag{16}$$

with $\mathcal{K}^{\mathbf{m}'}_{\mathbf{b}^{\mathbf{m}'}} \equiv \langle \tilde{\mathbf{b}}^{\mathbf{m}'} | H | \bar{\Psi} \rangle$ and MCR[X_1] is the set of excluded MCs that are one-mode excited w.r.t. an included MC. The variational optimization of the constraint operators can be shown to be equivalent to a linear least squares (LLS) minimization of the time derivative of the $C^{\mathbf{m}'}_{\mathbf{b}^{\mathbf{m}'}}$ coefficients with $\mathbf{m}' \in \mathrm{MCR}[X_1]$[18].

An alternative choice of constraint, also introduced in Ref. 18, is one that keeps the one-mode density matrices block diagonal and thus makes the reference configuration a product of natural modals. The non-redundant matrix elements of the constraint operators for the resulting MCTDH[n,D] models are obtained by solving a small set of linear equations for

each mode,

$$\sum_{b^m} \left(\delta_{a^m b^m} \tilde{D}^m_{i^m i^m} - \tilde{D}^m_{a^m b^m} \right) \tilde{g}^m_{i^m b^m} = \tilde{F}^{m\,*}_{i^m a^m} - \tilde{F}^m_{a^m i^m} \ , \tag{17}$$

This choice of constraint is computationally much cheaper than the fully variational solution and, thus, the MCTDH[n,D] methods can be applied to quite large systems[18]. The downside is that Eq. (17) becomes singular if the natural population of one of the virtual modals becomes as large as the population of the occupied modal. This calls for regularization and the MCTDH[n,D] EOMs become difficult to integrate if population changes a lot between configurations.

2.3 Treating non-adiabatic dynamics

The wave function Ansätze presented thus far (Eqs. (1) and (13)) are able to describe an evolving wave packet on a single Born-Oppenheimer potential-energy surface (PES). However, in order to simulate non-adiabatic effects occuring in the presence of conical intersections, the MCTDH wave function must take the electronic degree of freedom into account[2,44]. There exist two different formulations of MCTDH for non-adiabatic dynamics, the *single-set* formalism[50,51] and the *multi-set* formalism[52,53]. The fundamental difference between the two is that in the single-set formalism the same time-dependent modal basis is used on all PESs,

$$|\bar{\Psi}\rangle_{\mathrm{SS}} = \sum_{u^1=1}^{n^1} \cdots \sum_{u^M=1}^{n^M} \sum_{I=1}^{N^I} C_{u^1 \ldots u^M I} \left(\prod_{m=1}^{M} \tilde{a}^{m\,\dagger}_{u^m} \right) a^\dagger_I \, |\mathrm{vac}\rangle \ . \tag{18}$$

Note that the "modals" of the electronic degree of freedom are time-independent because the full set is used. The single-set formalism is simple to implement, but has the drawback that many time-dependent modals are needed for reaching convergence if the wave packets on the different surfaces become very different. In the multi-set formalism, on the other hand, different modal bases are used on each surface which allows for a more compact representation

of the wave function.

$$|\bar{\Psi}\rangle_{\mathrm{MS}} = \sum_{I} |\bar{\Psi}_I\rangle \, |I\rangle \ , \tag{19}$$

with

$$|\bar{\Psi}_I\rangle = \sum_{u_I^1=1}^{n_I^1} \cdots \sum_{u_I^M=1}^{n_I^M} C^I_{u_I^1 \ldots u_I^M} \prod_{m=1}^{M} \tilde{a}^{m\,I\,\dagger}_{u_I^m} |\mathrm{vac}\rangle \ . \tag{20}$$

However, due to non-orthogonality between the different bases, $[\tilde{a}^{m\,I}_{u_I^m}, \tilde{a}^{m\,J\,\dagger}_{v_J^m}] \neq \delta_{u_I^m v_J^m}$, the EOMs become more complicated[2].

In this work, we use the single-set formalism for describing non-adiabatic dynamics within the MCTDH[n] framework. In order to include the same number of configurations in the wave packets on the different surfaces the electronic degree of freedom needs to be treated in a special way as described in section 3.

3 MR-MCTDH[n] through systematic extension of the configuration space

The MCTDH[n] wave function of Eq. (13) is based on a single reference state which is assumed to have high occupation during the entire propagation. This assumption breaks down when the wave function attains MR character due to e.g. double-well potentials or during a non-adiabatic transition from one electronic state to another described in the single-set formulation. In these cases higher excitation levels need to be included in the wave function in order to describe the time evolution correctly. However, in many such cases not all of the higher-level excitations are required or they are at least not equally important. The number of configurations can be reduced significantly if the multi-reference character can be ascribed to one (or a few selected) modes, $\mathbf{m}_{\mathrm{MR}}$. Thus, it is the hope that a much more balanced wave function, in terms of accuracy and computational effort, can be constructed using the MR extension as opposed to increasing the overall excitation level.

We can generally define MR-MCTDH[n] wave functions by using flexible ways of defining the employed excitation space. These strategies will, one way or another, lead to excitation-counting methods whose logic differs from the usual one of simply counting excitations out of a single reference. However, within this very flexible setup are some very simple variants, and these are the ones we will investigate in our computations and therefore describe first in the following. If the modes in the set $\mathbf{m}_{\mathrm{MR}}$ are specifically important we can construct a MR-MCTDH[n] wave function by not counting excitations of the MR modes ($\mathbf{m}_{\mathrm{MR}}$) when truncating MCR[I]. Thus, if $\mathbf{m}_{\mathrm{MR}} = \{m_{\mathrm{MR}}\}$ the MR-MCTDH[2] wave function will account for all 3-mode excitations that include m_{MR} (in addition to all the 1 and 2-mode excitations usually included). A schematic representation of the modal spaces in this MR-MCTDH[n] is shown in figure 1. Using this MR formulation, all states that are excited exclusively in

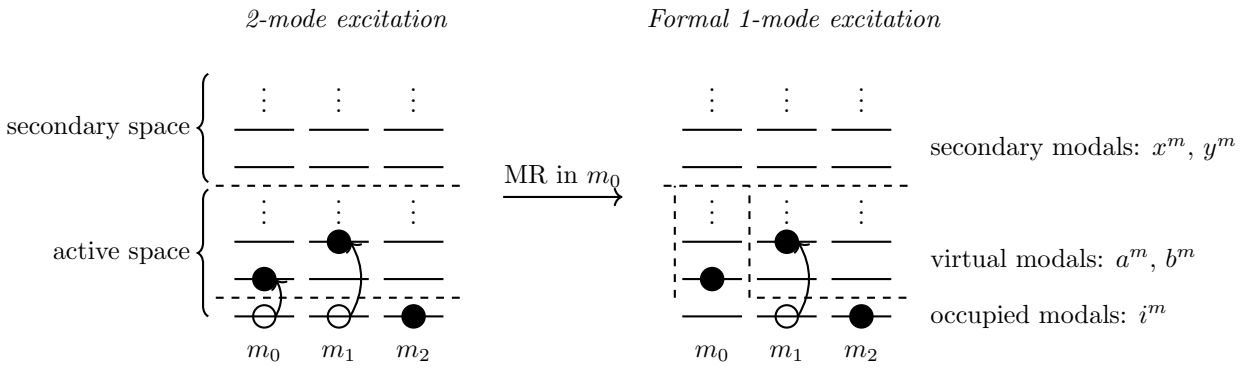

Figure 1: An example of MR-MCTDH[n] for a 3-mode system. The shown configuration is 2-mode excited w.r.t. the reference configuration when using regular single-reference MCTDH[n]. When using MR for mode m_0, all states that are 1-mode excited in mode m_0 are also treated as reference configurations and, thus, the shown configuration only counts as being 1-mode excited.

modes included in $\mathbf{m}_{\mathrm{MR}}$ are effectively also treated as reference configurations. Restricting the included MCs as in figure 1 gives a significant reduction in the scaling of computational effort in terms of the number of modes M compared to increasing the n-level of a standard MCTDH[n] to achieve inclusion of the same important configurations.

For many applications it is probably not necessary to treat all active-space excitations

within $\mathbf{m}_{\mathrm{MR}}$ as references. However, restricting the number of reference modals as shown in figure 2 will result in more complicated equations for determining the variationally optimal constraint operators (Eq. 14), as well as potentially leading to the need of different modal spaces for different MCs. Restrictions in the number of reference modals as outlined in

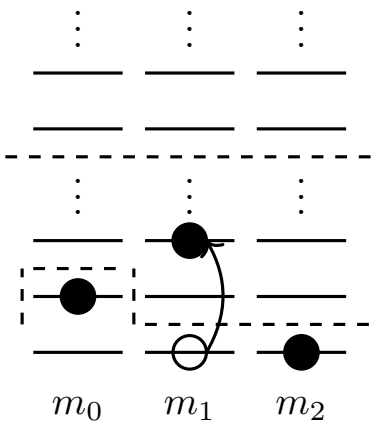

Figure 2: A MR scheme with further restrictions in the number of reference modals for the modes included in $\mathbf{m}_{\mathrm{MR}}$.

figure 2 will not give additional reductions in terms of M-scaling. Though some potential savings in absolute computational cost may be obtainable depending on the number of modes in $\mathbf{m}_{\mathrm{MR}}$, we choose, with reference to the above-mentioned unresolved theoretical problems, to only implement the scheme outlined in figure 1.

The MR method described here has some analogies to some methods in time-independent electronic structure theory, such as the restricted active space[54] and generalized active space[55] ideas in multi-configurational self-consistent field (MCSCF) and configuration interaction (CI) theory, as well as the sub-branch of multi-reference coupled cluster (MRCC) methods that are based on a single-reference (SR) formalism[56–58]. A topic of concern for the SR-based MRCC approach is that the MR configurations are *not* treated identically, as one of them has to be singled out as the formal reference. Accordingly, the model has difficulty describing states with vanishingly small weight for the chosen SR[58,59] unlike the situation for *genuine* MRCC schemes[59]. For the present purpose of MR-MCTDH[n], the weight of

the chosen reference is allowed to become zero in the wave function construction outlined above. Hence, we do not face the same problem as SR-based MRCC. Furthermore, with the modals evolving in time the reference has some flexibility to retain a high weight, as was observed in Ref. 18, especially for the MCTDH[n,D] methods. With this in mind, we expect the presented MR scheme to also be very useful in a TDVCC[24] context, particularly *if* the modals are time-dependent, although this will be the subject of a future study.

An important application of the MR formalism is to the single-set formalism for treating non-adiabatic dynamics discussed in section 2.3. In this case the electronic degree of freedom always needs to be included in $\mathbf{m}_{\mathrm{MR}}$ in order to include n-mode excitations of the vibrational wave function on all electronic states. Thus, when treating non-adiabatic dynamics, the configuration space of the given MCTDH[n] model is always extended in the electronic degree of freedom and we choose to omit the MR notation.

The concrete MR scheme discussed above can be viewed as a special case of a more general framework for constructing configuration spaces of many-mode systems. If each mode is assigned an excitation weight w^m, a flexible MCR can be built by only including MCs for which,

$$w^{\mathbf{m}} \equiv \sum_{m \in \mathbf{m}} w^m \leq n \; . \tag{21}$$

This can e.g. be applied to system-bath problems where higher excitation levels are required for the system (small w^m) and the bath can be treated using more approximate theory (large w^m). The MR-MCTDH[n] methods outlined by figure 1 are obtained by $w^m = 0$ for all $m \in \mathbf{m}_{\mathrm{MR}}$ and $w^m = 1$ for the remaining modes. The general excitation-weight framework is implemented in `MidasCpp`[60] and used as described with $w^m = 0$ or 1. Testing it in broader contexts is a subject for future investigation.

4 Implementation

The MCTDH methods described in section 2 have been implemented in the Molecular Interactions, Dynamics And Simulations Chemistry Program Package (MidasCpp)[60] which also includes an efficient implementation of TDH[3], TDVCC[24], as well as an array of methods for solving the TISE for molecular vibrations[21,23,61], tools for automatic generation of PESs and property surfaces[62–64], optimization of vibrational coordinates[65,66], etc. The time-independent wave-function methods are used to generate the initial wave packet which is propagated in time using the general-purpose routines described in Ref. 3. In this work we use the Dormand-Prince 8(5,3) explicit Runge-Kutta method[67] with adaptive step-size control for all calculations.

The MR-MCTDH[n] method is implemented by implementing Eq.(21) in the construction of MCR[I]. In all computations presented in section 5 $w^m = 0$ for the modes included in $\mathbf{m}_{\mathrm{MR}}$. Thereby, MCR[I] includes all MCs of dimension $\leq n$ and those MCs of up to $n + \dim(\mathbf{m}_{\mathrm{MR}})$ degrees of freedom which have one or more modes in $\mathbf{m}_{\mathrm{MR}}$.

5 Results

The following sections present numerical results for MCTDH[n] and MR-MCTDH[n] calculations on the formyl fluoride PES presented in Ref. 18, the 6D and 13D salicylaldimine PESs of Ref. 68, and the 4D and 24D pyrazine models of Ref. 69. For formyl fluoride the intramolecular vibrational-energy redistribution (IVR) from an initially excited C-H stretch is studied in terms of the decay of the autocorrelation function. The salicylaldimine models are used for studying the flux over the transition state, and for pyrazine the photoabsorption spectrum and diabatic state populations are calculated.

The number of configurations in the MR and SR MCTDH[n] wave functions used for studying these systems are shown in table 2. For (MR-)MCTDH[n] the number of configurations is in general a good measure for the computational cost of a given calculation,

although the choice of constraint also matters with (MR-)MCTDH[n,V] being the most expensive methods. We note that this is not necessarily the case for other types of methods such as ML-MCTDH where the EOMs for the wave-function parameters of the different layers are interdependent and the cost per parameter may become significantly higher than in standard MCTDH. Concrete timings for a series of calculations on 6D salicylaldimine are shown in table 3. These confirm that for each choice of constraint the cost of a MR-MCTDH[n] calculation lies between the those of MCTDH[n] and MCTDH[$n+1$]. The MR-MCTDH[4,V] calculation is slightly more expensive than full MCTDH due to the low dimensionality of the system, but as shown later in figure 4 the flux is converged already at the MR-MCTDH[3,V] level.

Table 2: Number of configurations included in the MR and SR MCTDH[n] wave functions used for studying the formyl fluoride molecule, the 6D and 13D salicylaldimine models, and the 4D and 24D pyrazine models. Note that the full MCTDH calculations on the 13D salicylaldimine and the 24D pyrazine models have not been performed.

	n	2	3	4	Full
Formyl fluoride and	$N^{\mathrm{SR}}_{\mathrm{config}}$	406	2906	12 281	46 656
6D salicylaldimine	$N^{\mathrm{MR}}_{\mathrm{config}}$	1656	9156	27 906	
13D salicylaldimine	$N^{\mathrm{SR}}_{\mathrm{config}}$	2016	37 766	484 641	13 060 694 016
	$N^{\mathrm{MR}}_{\mathrm{config}}$	10 266	175 266	2 031 516	
4D pyrazine	N_{config}	1344	9240	26 880	26 880
24D pyrazine	N_{config}	19 444	837 140	25 646 130	98 277 538 868 892 794 880

5.1 Computational details

The time-independent basis sets used for the wave-packet propagations are harmonic-oscillator basis functions (using ground-state normal-mode frequencies) for pyrazine and a B-spline basis for formyl fluoride. For salicylaldimine a B-spline basis is used for treating the double-well mode and harmonic-oscillator functions are used for the rest. Both types of basis functions are transformed to a set of orthonormal vibrational self-consistent field (VSCF) modals before starting the propagation. The initial wave packets are generated using the VSCF module of MidasCpp. The time-dependent modals of the active space are initially chosen as

Table 3: Time (in seconds) per derivative evaluation for a series of MR and SR MCTDH[n] calculations performed on 6D salicylaldimine.

Model	$t^{\mathrm{SR}}_{\mathrm{deriv}}$	$t^{\mathrm{MR}}_{\mathrm{deriv}}$
[2,g0]	1.40×10^{-2}	2.30×10^{-2}
[2,D]	1.45×10^{-2}	2.41×10^{-2}
[2,V]	2.19×10^{-2}	3.90×10^{-2}
[3,g0]	3.28×10^{-2}	7.46×10^{-3}
[3,D]	3.24×10^{-2}	7.51×10^{-2}
[3,V]	5.88×10^{-2}	1.15×10^{-1}
[4,g0]	9.41×10^{-2}	2.03×10^{-1}
[4,D]	9.47×10^{-2}	2.06×10^{-1}
[4,V]	1.53×10^{-1}	2.64×10^{-1}
MCTDH	2.37×10^{-1}	

the n^m lowest-energy VSCF modals for each mode. For a harmonic potential (such as the electronic ground state of the pyrazine models) this results in a harmonic-oscillator basis, while anharmonicity is incorporated in the initial modals for other types of PESs.

Spectra are calculated by performing fast Fourier transform (FFT) on the autocorrelation function defined as,

$$S(t) = \langle \bar{\Psi}(0) | \bar{\Psi}(t) \rangle = \langle \bar{\Psi}^*(t/2) | \bar{\Psi}(t/2) \rangle \ , \tag{22}$$

where the last equality only holds if $\bar{\Psi}^*(0) = \bar{\Psi}(0)$ and $H = H^T$[2]. In order to introduce phenomenological broadening of the spectra, the autocorrelation function can be modified as,

$$\tilde{S}(t) = S(t) \exp\left(-\frac{|t|}{\tau}\right) \ , \tag{23}$$

where τ is a given lifetime.

For salicylaldimine the flux over the transition state is calculated as the expectation value of the flux operator[2],

$$F_{Q_1=0} = i[H, \Theta(Q_1)] = -\frac{i}{2}\left(\frac{\partial}{\partial Q_1}\delta(Q_1) + \delta(Q_1)\frac{\partial}{\partial Q_1}\right) \ , \tag{24}$$

where $\Theta(Q_1)$ is the Heaviside step function, $\delta(Q_1)$ is the Dirac delta function, and the last

equality only holds in recitilinear coordinates where the kinetic-energy operator is of the form $T_{m_1} = -\frac{1}{2}\frac{\partial^2}{\partial {Q_1}^2}$.

5.2 Intramolecular vibrational-energy redistribution

We first study the IVR of formyl fluoride using MR-MCTDH[n] with the initially excited C-H stretch as the MR mode. As in Ref. 18 the initial wave packet is generated by performing a VSCF calculation targeting the [0,0,0,0,0,2] state (the C-H stretch) on a PES with all the coupling terms removed, i.e. a set of uncoupled anharmonic oscillators. The MCTDH calculations are performed using $n^m = 6$ in all modes in order to compare directly with the results of Ref. 18 (initial tests were performed to ensure that $n^m = 6$ is sufficient). Figure 3 shows the decay of the autocorrelation function as well as the difference between the MCTDH and MR-MCTDH[n] results. The results clearly show that the MR wave functions converge fast towards full MCTDH and already at the MR-MCTDH[2,V] level the autocorrelation functions are very similar. In fact, the MR-MCTDH[2] results qualitatively correspond to the MCTDH[3] results in Ref. 18, signifying that the MR scheme succeeds in including the most relevant 3-mode excitations. Note that the MCTDH[3] wave function includes almost twice as many configurations as the MR-MCTDH[2] wave function (2906 vs. 1656). In contrast the single-reference MCTDH[2] results shown in Ref. 18 do not reproduce the correct decay of the autocorrelation function, and thus using a MR description of the C-H stretch greatly improves convergence of the MCTDH[n] hierarchy.

5.3 Double-well system

We now turn to studying the proton-transfer reaction of the salicylaldimine molecule. The PES contains an asymmetric double well (in the mode denoted as m_1) which is expected to lead to MR character in the wave function. As in Ref. 68 the initial wave packets are generated as Gaussian functions with widths corresponding to the enol widths shown in table 4. The initial position expectation values of the wave packets are $\langle Q_1 \rangle = 0.9634$,

$\langle Q_{36} \rangle = 0.1373$, and $\langle Q \rangle = 0$ for the remaining modes (in mass-frequency-scaled normal coordinates). As the zero for the coordinates is at the transition state, this places the wave packet close to the barrier on the slope towards the more stable enol conformation, but with an energy less than the barrier height (see Ref. 68 for details and illustrations of the normal modes and PES). We examine both the 13D model using all modes in table 4 and the 6D model which includes the following modes: m_1, m_{10}, m_{11}, m_{13}, m_{32}, and m_{36}. The

Table 4: Position expectation values and relaxed wave-packet widths ($\Delta Q = \sqrt{\langle Q^2 \rangle - \langle Q \rangle^2}$) of the enol conformation of salicylaldimine (from Ref. 68).

	m_1	m_5	m_7	m_9	m_{10}	m_{11}	m_{13}	m_{16}	m_{22}	m_{23}	m_{24}	m_{32}	m_{36}
$\langle Q \rangle$	2.3903	0.7196	0.6020	0.5752	-1.5657	-1.0808	0.8422	0.3082	-0.2273	-0.0826	-0.3140	0.2421	0.6045
ΔQ	0.5706	0.7409	0.7150	0.7115	0.7745	0.7590	0.6902	0.7167	0.7139	0.7166	0.7154	0.6707	0.7704

wave packets were propagated to $t = 4200\,\text{au} \simeq 100\,\text{fs}$ using 6 time-dependent modals in all modes. Figure 4 shows the flux over the transition state of the 6D model using different (MR-)MCTDH[n,g0], (MR-)MCTDH[n,D], and (MR-)MCTDH[n,V] models, respectively. The same results for the 13D model are shown in figure 5. The results clearly show that a MR description of the double-well mode is essential for obtaining correct results at low excitation levels. Among the MCTDH[2] models only the MR-MCTDH[2,D] and MR-MCTDH[2,V] methods produce qualitatively correct results after the initial barrier crossing. The single-reference MCTDH[2] methods all result in unstable propagation and even qualitatively wrong flux at longer times. For the 6D model, all methods are seen to converge towards the full MCTDH results when going to higher excitation levels and at the MCTDH[4] level all except the MCTDH[4,g0] and MR-MCTDH[4,g0] methods are virtually indistinguishable from full MCTDH. For the 13D model the same trends are observed. The flux calculated by MR-MCTDH[2,D] and MR-MCTDH[2,V] is essentially converged until right before the final crossing (starting at $\sim 2400\,\text{au}$). On the other hand, the single-reference MCTDH[2] methods are not even able to predict the correct flux of the first recrossing occuring between 300 and 1000 au.

5.4 Non-adiabatic dynamics

We finally study the non-adiabatic dynamics of the pyrazine molecule using the 4D and 24D models of Ref. 69. The number of time-dependent modals is (as suggested in Ref. 2) ($n^{\nu_{10a}}$, $n^{\nu_{6a}}$, n^{ν_1}, $n^{\nu_{9a}}$) = (16, 15, 8, 7) and for the 24D model we use $n^m = 6$ for the remaining modes. The initial wave packets were generated as Gaussian functions using the normal-mode frequencies of the electronic ground state and placed on the S2 surface. The 4D system was propagated to $t = 10^4$ au $\simeq 242$ fs and the 24D system was propagated to $t = 6200$ au $\simeq 150$ fs. Only the MCTDH[n,g0] and MCTDH[n,V] results are compared as the MCTDH[n,D] wave functions became very difficult to propagate due to the large changes in occupation numbers caused by the non-adiabatic dynamics. Recall that the electronic degree of freedom is always treated as an MR mode although this is not explicitly reflected in the notation. Figure 6 shows photoabsorption spectra and diabatic state populations of the 4D pyrazine model. The corresponding results for the 24D model are shown in figure 7.

For both models it becomes clear that the fully variational MCTDH[n,V] hierarchy converges much faster than the corresponding MCTDH[n,g0] wave functions. For the 4D model, the MCTDH[3,V] results are basically converged (as expected) while this is not the case for MCTDH[3,g0]. For the full 24D model all the MCTDH[n,V] methods produce qualitatively correct spectra and the state populations for MCTDH[3,V] and MCTDH[4,V] are very similar during the first ~ 2000 au of the propagation. Most importantly, the dynamics leading up to the crossing between the diabatic populations is converged already at the MCTDH[3,V] level.

6 Summary and outlook

A MR extension to the MCTDH[n] hierarchy has been introduced which includes selected higher-order excitations for the modes that govern the quantum dynamics of the system. This is formally equivalent to treating all configurations that are excited exclusively in the

MR modes as reference configurations. The MR-MCTDH[n] methods are implemented by simply modifying the MCR of included configurations, MCR[I], and thus the various choices of constraint operators outlined in section 2.2 can be straightforwardly employed.

The MR formalism has been applied to studying the IVR of formyl fluoride, the proton-transfer reaction of salicylaldimine, and the non-adiabatic dynamics of pyrazine. The numerical results show that the MR-MCTDH[n] methods provide a more balanced description of the studied systems compared to single-reference MCTDH[n] and ensure fast convergence towards the full MCTDH limit. As expected, the choice of constraint operators is key to obtaining accurate results at low excitation levels. For the formyl fluoride and salicylaldimine calculations the MR-MCTDH[n,D] and MR-MCTDH[n,V] hierarchies converge fast towards the full MCTDH limit compared to MR-MCTDH[n,g0]. For the non-adiabatic dynamics of pyrazine the density-matrix constraint resulted in very small integration steps close to the point where the diabatic populations of the two electronic states cross. This exemplifies that while the density-matrix and the fully variational constraints typically lead to similar accuracy, the MCTDH[n,V] EOMs are numerically more stable.

In this work we have exclusively used the single-set formalism for treating non-adiabatic dynamics within the MCTDH framework. However, in order to further reduce the required number of time-dependent modals a formulation and implementation of MCTDH[n] within the multi-set formalism could be an important step towards studying the complex photodynamics of larger molecules. Also, applying the general excitation-weight framework outlined in section 3 to studying system-bath problems with MCTDH[n] is a relevant topic for future investigation. Furthermore, a (semi-)automated scheme for identifying the MR modes will be an important tool for applying MR-MCTDH[n] to larger and more complex systems. Such a procedure could e.g. be based on norms of the coefficients of the 1-mode excitations in a SR MCTDH[n] calculation, but this approach remains to be studied further. Finally, developing a scheme for dynamically including the relevant couplings in the wave function during the course of propagation while keeping the required number of configurations small

is an important subject for future research in this area.

Acknowledgements

O.C. acknowledges support from the Danish Council for Independent Research through a Sapere Aude III grant (DFF - 4002-00015), the Lundbeck Foundation, and the Danish e-infrastructure Cooperation (DeiC).

References

(1) Meyer, H.-D.; Manthe, U.; Cederbaum, L. S. The multi-configurational time-dependent Hartree approach. *Chem. Phys. Lett.* **1990**, *165*, 73 – 78.

(2) Beck, M.; Jackle, A.; Worth, G.; Meyer, H. The multiconfiguration time-dependent Hartree (MCTDH) method: a highly efficient algorithm for propagating wavepackets. *Phys. Rep.* **2000**, *324*, 1–105.

(3) Madsen, N. K.; Hansen, M. B.; Zoccante, A.; Monrad, K.; Hansen, M. B.; Christiansen, O. Exponential parameterization of wave functions for quantum dynamics: Time-dependent Hartree in second quantization. *J. Chem. Phys.* **2018**, *149*, 134110.

(4) Makri, N. Time Dependent Quantum Methods for Large Systems. *Annu. Rev. Phys. Chem.* **1999**, *50*, 167–191.

(5) Wang, H.; Thoss, M. Multilayer formulation of the multiconfiguration time-dependent Hartree theory. *J. Chem. Phys.* **2003**, *119*, 1289–1299.

(6) Wang, H.; Thoss, M. Numerically exact quantum dynamics for indistinguishable particles: The multilayer multiconfiguration time-dependent Hartree theory in second quantization representation. *J. Chem. Phys.* **2009**, *131*, 024114.

(7) Manthe, U. A multilayer multiconfigurational time-dependent Hartree approach for quantum dynamics on general potential energy surfaces. *J. Chem. Phys.* **2008**, *128*, 164116.

(8) Vendrell, O.; Meyer, H.-D. Multilayer multiconfiguration time-dependent Hartree method: Implementation and applications to a Henon-Heiles Hamiltonian and to pyrazine. *J. Chem. Phys.* **2011**, *134*, 044135.

(9) Burghardt, I.; Meyer, H.; Cederbaum, L. Approaches to the approximate treatment of complex molecular systems by the multiconfiguration time-dependent Hartree method. *J. Chem. Phys.* **1999**, *111*, 2927.

(10) Burghardt, I.; Giri, K.; Worth, G. A. Multimode quantum dynamics using Gaussian wavepackets: The Gaussian-based multiconfiguration time-dependent Hartree (G-MCTDH) method applied to the absorption spectrum of pyrazine. *J. Chem. Phys.* **2008**, *129*, 174104.

(11) Worth, G. A.; Burghardt, I. Full quantum mechanical molecular dynamics using Gaussian wavepackets. *Chem. Phys. Lett.* **2003**, *368*, 502 – 508.

(12) Richings, G.; Polyak, I.; Spinlove, K.; Worth, G.; Burghardt, I.; Lasorne, B. Quantum dynamics simulations using Gaussian wavepackets: the vMCG method. *Int. Rev. Phys. Chem.* **2015**, *34*, 269–308.

(13) Shalashilin, D. V.; Child, M. S. Multidimensional quantum propagation with the help of coupled coherent states. *J. Chem. Phys.* **2001**, *115*, 5367–5375.

(14) Green, J. A.; Grigolo, A.; Ronto, M.; Shalashilin, D. V. A two-layer approach to the coupled coherent states method. *J. Chem. Phys.* **2016**, *144*, 024111.

(15) Ben-Nun, M.; Martínez, T. Nonadiabatic molecular dynamics: Validation of the mul-

tiple spawning method for a multidimensional problem. *J. Chem. Phys.* **1998**, *108*, 7244.

(16) Ben-Nun, M.; Quenneville, J.; Martinez, T. Ab initio multiple spawning: Photochemistry from first principles quantum molecular dynamics. *J. Phys. Chem. A* **2000**, *104*, 5161–5175.

(17) Curchod, B. F. E.; Martínez, T. J. Ab Initio Nonadiabatic Quantum Molecular Dynamics. *Chem. Rev.* **2018**, *118*, 3305–3336.

(18) Madsen, N. K.; Hansen, M. B.; Worth, G. A.; Christiansen, O. Systematic and variational truncation of the configuration space in the multiconfiguration time-dependent Hartree method: The MCTDH[n] hierarchy. *J. Chem. Phys.* **2020**, *152*, 084101.

(19) Christiansen, O. A second quantization formulation of multimode dynamics. *J. Chem. Phys.* **2004**, *120*, 2140.

(20) Christiansen, O. Vibrational structure theory: new vibrational wave function methods for calculation of anharmonic vibrational energies and vibrational contributions to molecular properties. *Phys. Chem. Chem. Phys.* **2007**, *9*, 2942.

(21) Christiansen, O. Vibrational coupled cluster theory. *J. Chem. Phys* **2004**, *120*, 2149.

(22) Seidler, P.; Christiansen, O. Automatic derivation and evaluation of vibrational coupled cluster theory equations. *J. Chem. Phys.* **2009**, *131*, 234109.

(23) Madsen, N. K.; Godtliebsen, I. H.; Losilla, S. A.; Christiansen, O. Tensor-decomposed vibrational coupled-cluster theory: Enabling large-scale, highly accurate vibrational-structure calculations. *J. Chem. Phys.* **2018**, *148*, 024103.

(24) Hansen, M. B.; Madsen, N. K.; Zoccante, A.; Christiansen, O. Time-dependent vibrational coupled cluster theory: Theory and implementation at the two-mode coupling level. *J. Chem. Phys.* **2019**, *151*, 154116.

(25) Worth, G. A. Accurate wave packet propagation for large molecular systems: The multi-configuration time-dependent Hartree (MCTDH) method with selected configurations. *J. Chem. Phys* **2000**, *112*, 8322–8329.

(26) Wodraszka, R.; Carrington, T. Using a pruned, nondirect product basis in conjunction with the multi-configuration time-dependent Hartree (MCTDH) method. *J. Chem. Phys.* **2016**, *145*, 044110.

(27) Wodraszka, R.; Carrington, T. Systematically expanding nondirect product bases within the pruned multi-configuration time-dependent Hartree (MCTDH) method: A comparison with multi-layer MCTDH. *J. Chem. Phys.* **2017**, *146*, 194105.

(28) Larsson, H. R.; Tannor, D. J. Dynamical pruning of the multiconfiguration time-dependent Hartree (DP-MCTDH) method: An efficient approach for multidimensional quantum dynamics. *J. Chem. Phys.* **2017**, *147*, 044103.

(29) McCormack, D. A. Dynamical pruning of static localized basis sets in time-dependent quantum dynamics. *J. Chem. Phys.* **2006**, *124*, 204101.

(30) Habershon, S. Trajectory-guided configuration interaction simulations of multidimensional quantum dynamics. *J. Chem. Phys.* **2012**, *136*, 054109.

(31) Machnes, S.; Assémat, E.; Larsson, H. R.; Tannor, D. J. Quantum Dynamics in Phase Space using Projected von Neumann Bases. *J. Phys. Chem. A* **2016**, *120*, 3296–3308.

(32) Larsson, H. R.; Hartke, B.; Tannor, D. J. Efficient molecular quantum dynamics in coordinate and phase space using pruned bases. *J. Chem. Phys.* **2016**, *145*, 204108.

(33) Yang, W.; Peet, A. C. A method for calculating vibrational bound states: Iterative solution of the collocation equations constructed from localized basis sets. *J. Chem. Phys.* **1990**, *92*, 522–526.

(34) Cooper, J.; Carrington, T. Computing vibrational energy levels by using mappings to fully exploit the structure of a pruned product basis. *J. Chem. Phys.* **2009**, *130*, 214110.

(35) Avila, G.; Carrington, T. Using a pruned basis, a non-product quadrature grid, and the exact Watson normal-coordinate kinetic energy operator to solve the vibrational Schrödinger equation for C $_2$ H $_4$. *J. Chem. Phys.* **2011**, *135*, 064101.

(36) Avila, G.; Carrington, T. Solving the vibrational Schrödinger equation using bases pruned to include strongly coupled functions and compatible quadratures. *J. Chem. Phys.* **2012**, *137*, 174108.

(37) Brown, J.; Carrington, T. Using an expanding nondirect product harmonic basis with an iterative eigensolver to compute vibrational energy levels with as many as seven atoms. *J. Chem. Phys.* **2016**, *145*, 144104.

(38) Avila, G.; Carrington, T. Pruned bases that are compatible with iterative eigensolvers and general potentials: New results for CH3CN. *Chem. Phys.* **2017**, *482*, 3 – 8.

(39) Miyagi, H.; Madsen, L. B. Time-dependent restricted-active-space self-consistent-field theory for laser-driven many-electron dynamics. *Phys. Rev. A* **2013**, *87*.

(40) Miyagi, H.; Madsen, L. B. Time-dependent restricted-active-space self-consistent-field theory for laser-driven many-electron dynamics. II. Extended formulation and numerical analysis. *Phys. Rev. A* **2014**, *89*.

(41) Haxton, D. J.; McCurdy, C. W. Two methods for restricted configuration spaces within the multiconfiguration time-dependent Hartree-Fock method. *Phys. Rev. A* **2015**, *91*.

(42) Lévêque, C.; Madsen, L. B. Time-dependent restricted-active-space self-consistent-field theory for bosonic many-body systems. *New J. Phys.* **2017**, *19*, 043007.

(43) Manthe, U. Comment on "A multiconfiguration time-dependent Hartree approximation

based on natural single-particle states" [J. Chem. Phys. **99** , 4055 (1993)]. *J. Chem. Phys.* **1994**, *101*, 2652–2653.

(44) Worth, G. A.; Meyer, H.-D.; Köppel, H.; Cederbaum, L. S.; Burghardt, I. Using the MCTDH wavepacket propagation method to describe multimode non-adiabatic dynamics. *Int. Rev. Phys. Chem.* **2008**, *27*, 569–606.

(45) Alon, O. E.; Streltsov, A. I.; Cederbaum, L. S. Unified view on multiconfigurational time propagation for systems consisting of identical particles. *J. Chem. Phys.* **2007**, *127*, 154103.

(46) Alon, O. E.; Streltsov, A. I.; Cederbaum, L. S. Multiconfigurational time-dependent Hartree method for bosons: Many-body dynamics of bosonic systems. *Phys. Rev. A* **2008**, *77*, 033613.

(47) Wang, H.; Thoss, M. Numerically exact quantum dynamics for indistinguishable particles: The multilayer multiconfiguration time-dependent Hartree theory in second quantization representation. *J. Chem. Phys.* **2009**, *131*, 024114.

(48) Manthe, U.; Weike, T. On the multi-layer multi-configurational time-dependent Hartree approach for bosons and fermions. *J. Chem. Phys.* **2017**, *146*, 064117.

(49) Weike, T.; Manthe, U. The multi-configurational time-dependent Hartree approach in optimized second quantization: Imaginary time propagation and particle number conservation. *J. Chem. Phys.* **2020**, *152*, 034101.

(50) Manthe, U.; Hammerich, A. D. Wavepacket dynamics in five dimensions. Photodissociation of methyl iodide. *Chem. Phys. Lett.* **1993**, *211*, 7 – 14.

(51) Hammerich, A. D.; Manthe, U.; Kosloff, R.; Meyer, H.-D.; Cederbaum, L. S. Time-dependent photodissociation of methyl iodide with five active modes. *J. Chem. Phys.* **1994**, *101*, 5623–5646.

(52) Fang, J.-Y.; Guo, H. Multiconfiguration time-dependent Hartree studies of the CH_3I/MgO photodissociation dynamics. *J. Chem. Phys.* **1994**, *101*, 5831–5840.

(53) Worth, G. A.; Meyer, H.-D.; Cederbaum, L. S. The effect of a model environment on the S_2 absorption spectrum of pyrazine: A wave packet study treating all 24 vibrational modes. *J. Chem. Phys.* **1996**, *105*, 4412–4426.

(54) Olsen, J.; Roos, B. O.; Jørgensen, P.; Jensen, H. J. A. Determinant based configuration interaction algorithms for complete and restricted configuration interaction spaces. *J. Chem. Phys.* **1988**, *89*, 2185–2192.

(55) Fleig, T.; Olsen, J.; Marian, C. M. The generalized active space concept for the relativistic treatment of electron correlation. I. Kramers-restricted two-component configuration interaction. *J. Chem. Phys.* **2001**, *114*, 4775–4790.

(56) Piecuch, P.; Oliphant, N.; Adamowicz, L. A state-selective multireference coupled-cluster theory employing the single-reference formalism. *J. Chem. Phys.* **1993**, *99*, 1875–1900.

(57) Olsen, J. The initial implementation and applications of a general active space coupled cluster method. *J. Chem. Phys.* **2000**, *113*, 7140–7148.

(58) Kállay, M.; Szalay, P. G.; Surján, P. R. A general state-selective multireference coupled-cluster algorithm. *J. Chem. Phys.* **2002**, *117*, 980–990.

(59) Köhn, A.; Hanauer, M.; Mück, L. A.; Jagau, T.-C.; Gauss, J. State-specific multireference coupled-cluster theory. *Wiley Interdiscip. Rev.: Comput. Mol. Sci.* **2013**, *3*, 176–197.

(60) Christiansen, O.; Artiukhin, D.; Godtliebsen, I. H.; Gras, E. M.; Győrffy, W.; Hansen, M. B.; Hansen, M. B.; Kongsted, J.; Klinting, E. L.; König, C.; Losilla, S. A.;

Madsen, D.; Madsen, N. K.; Monrad, K.; Seidler, P.; Sneskov, K.; Sparta, M.; Thomsen, B.; Toffoli, D.; Zoccante, A. *MidasCpp (Molecular Interactions, dynamics and simulation Chemistry program package in C++)*; 2020; https://midascpp.gitlab.io/.

(61) Hansen, M.; Sparta, M.; Seidler, P.; Toffoli, D.; Christiansen, O. New Formulation and Implementation of Vibrational Self-Consistent Field Theory. *J. Chem. Theory Comput.* **2010**, *6*, 235–248.

(62) Sparta, M.; Toffoli, D.; Christiansen, O. An Adaptive Density-Guided Approach for the Generation of Potential Energy Surfaces of Polyatomic Molecules. *Theor. Chem. Acc.* **2009**, *123*, 413–429.

(63) Klinting, E. L.; Thomsen, B.; Godtliebsen, I. H.; Christiansen, O. Employing general fit-bases for construction of potential energy surfaces with an adaptive density-guided approach. *J. Chem. Phys.* **2018**, *148*, 064113.

(64) König, C.; Christiansen, O. Linear-scaling generation of potential energy surfaces using a double incremental expansion. *J. Chem. Phys.* **2016**, *145*, 064105.

(65) Thomsen, B.; Yagi, K.; Christiansen, O. A simple state-average procedure determining optimal coordinates for anharmonic vibrational calculations. *Chem. Phys. Lett.* **2014**, *610-611*, 288 – 297.

(66) Klinting, E. L.; König, C.; Christiansen, O. Hybrid Optimized and Localized Vibrational Coordinates. *J. Phys. Chem. A* **2015**, *119*, 11007–11021.

(67) Hairer, E.; Wanner, G.; Nørsett, S. P. *Solving Ordinary Differential Equations I: Non-stiff Problems*; Springer, 1993.

(68) Polyak, I.; Allan, C. S. M.; Worth, G. A. A complete description of tunnelling using direct quantum dynamics simulation: Salicylaldimine proton transfer. *J. Chem. Phys.* **2015**, *143*, 084121.

(69) Raab, A.; Worth, G. A.; Meyer, H.-D.; Cederbaum, L. S. Molecular dynamics of pyrazine after excitation to the S2 electronic state using a realistic 24-mode model Hamiltonian. *J. Chem. Phys.* **1999**, *110*, 936–946.

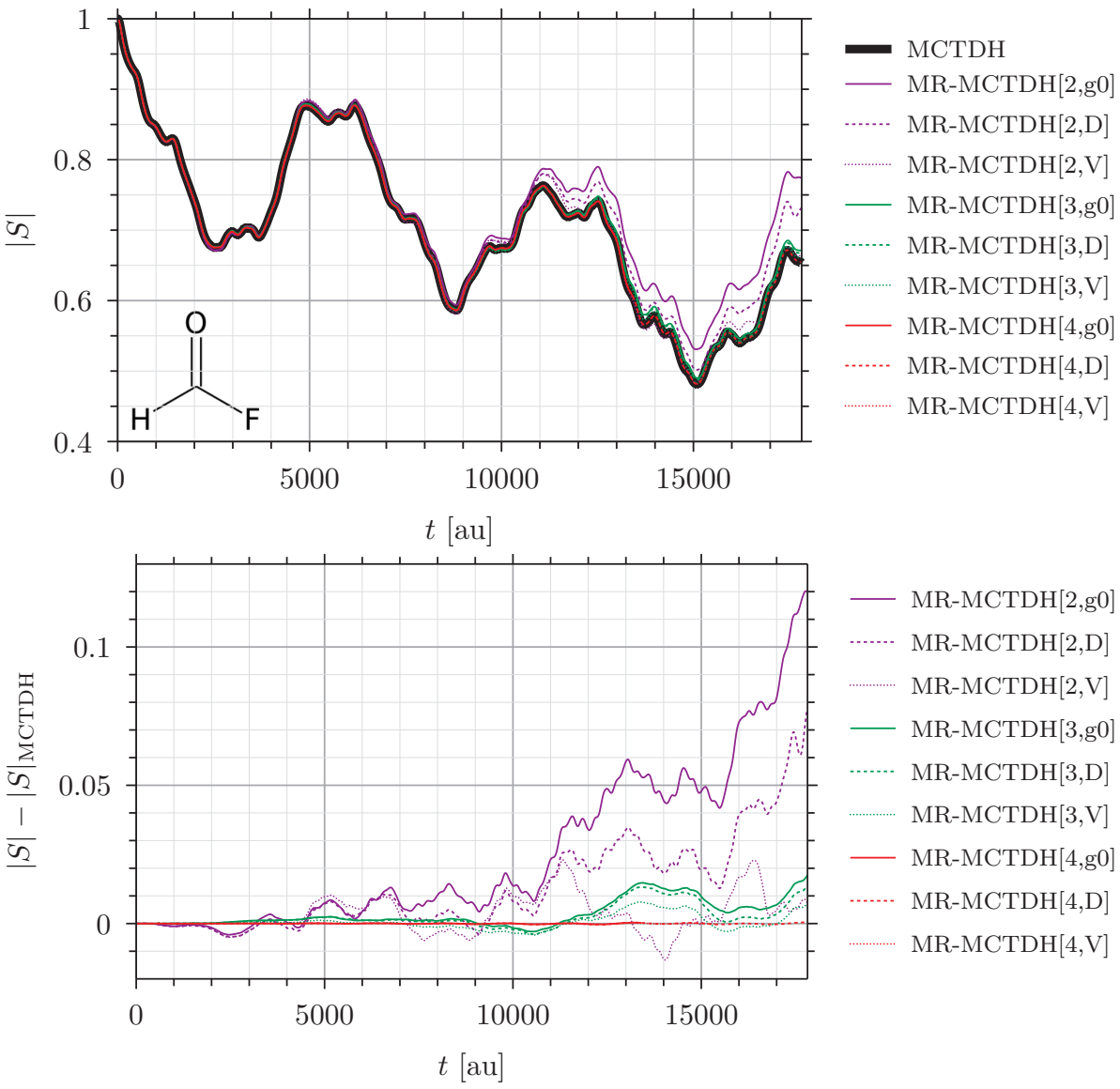

Figure 3: Top: Absolute value of the autocorrelation function for formyl fluoride. Bottom: Difference between the full MCTDH and MR-MCTDH[n] autocorrelation functions.

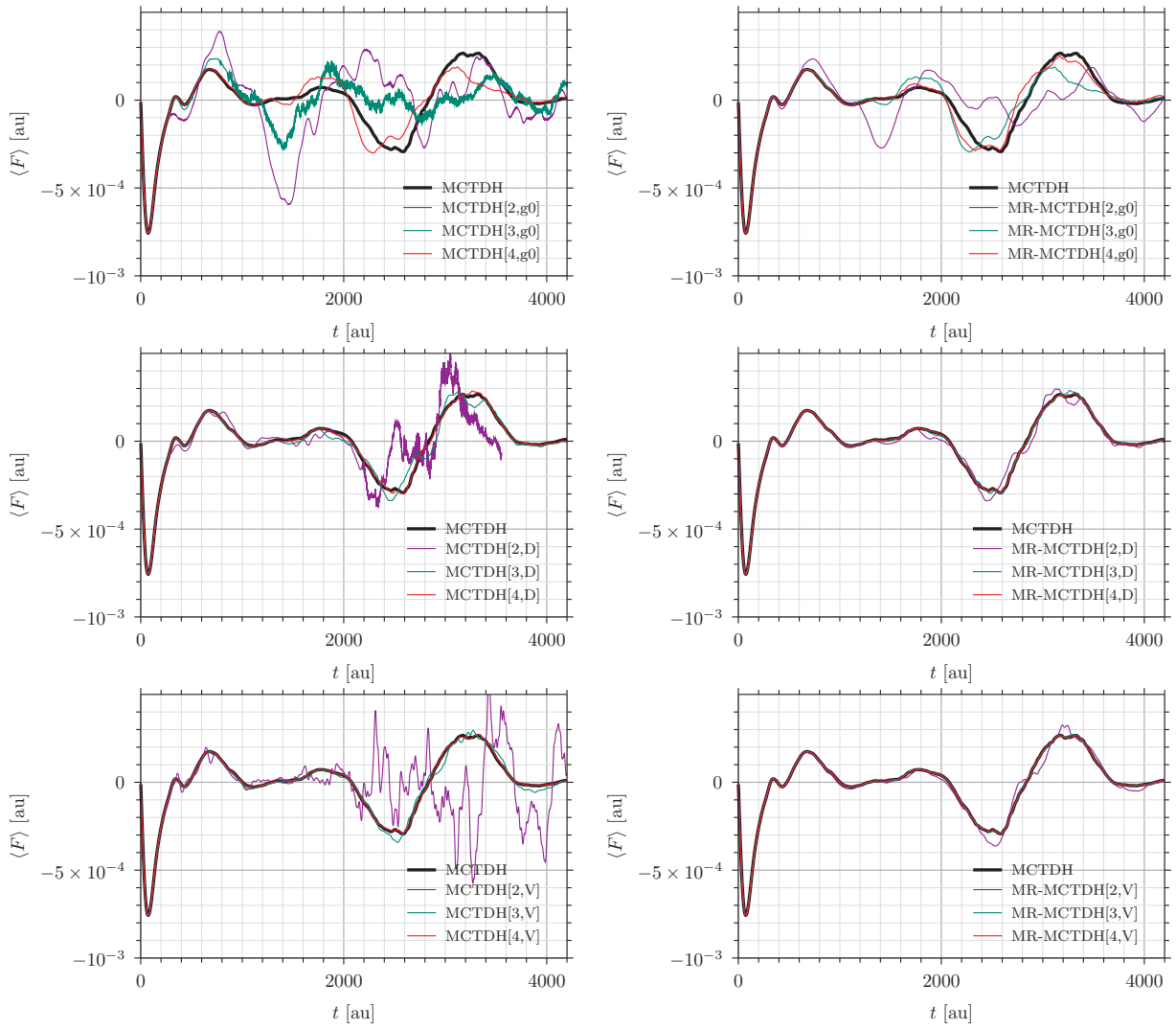

Figure 4: Flux over the transition state of the 6D salicylaldimine potential for MCTDH[n] (left) and MR-MCTDH[n] (right).

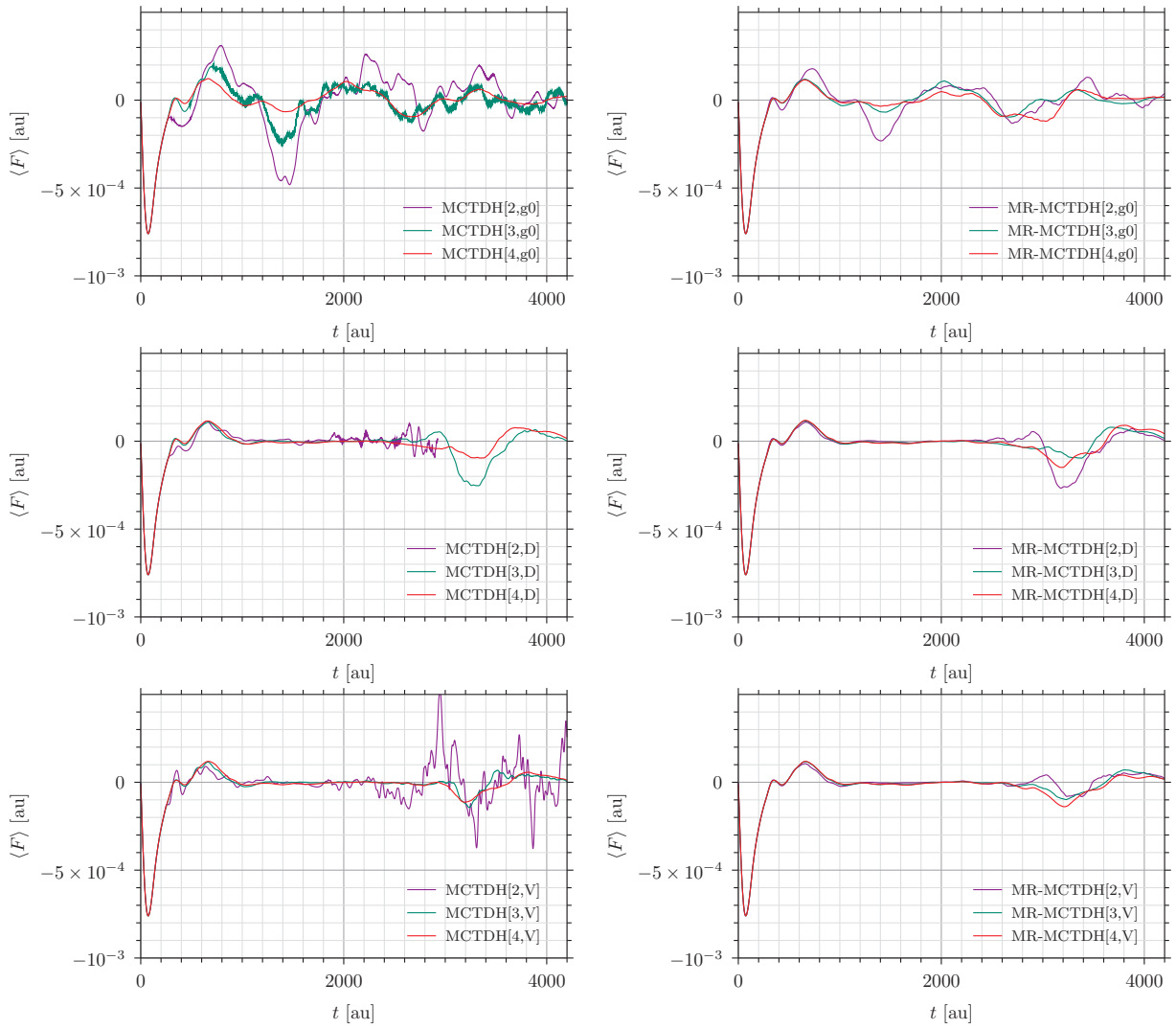

Figure 5: Flux over the transition state of the 13D salicylaldimine potential for MCTDH[n] (left) and MR-MCTDH[n] (right).

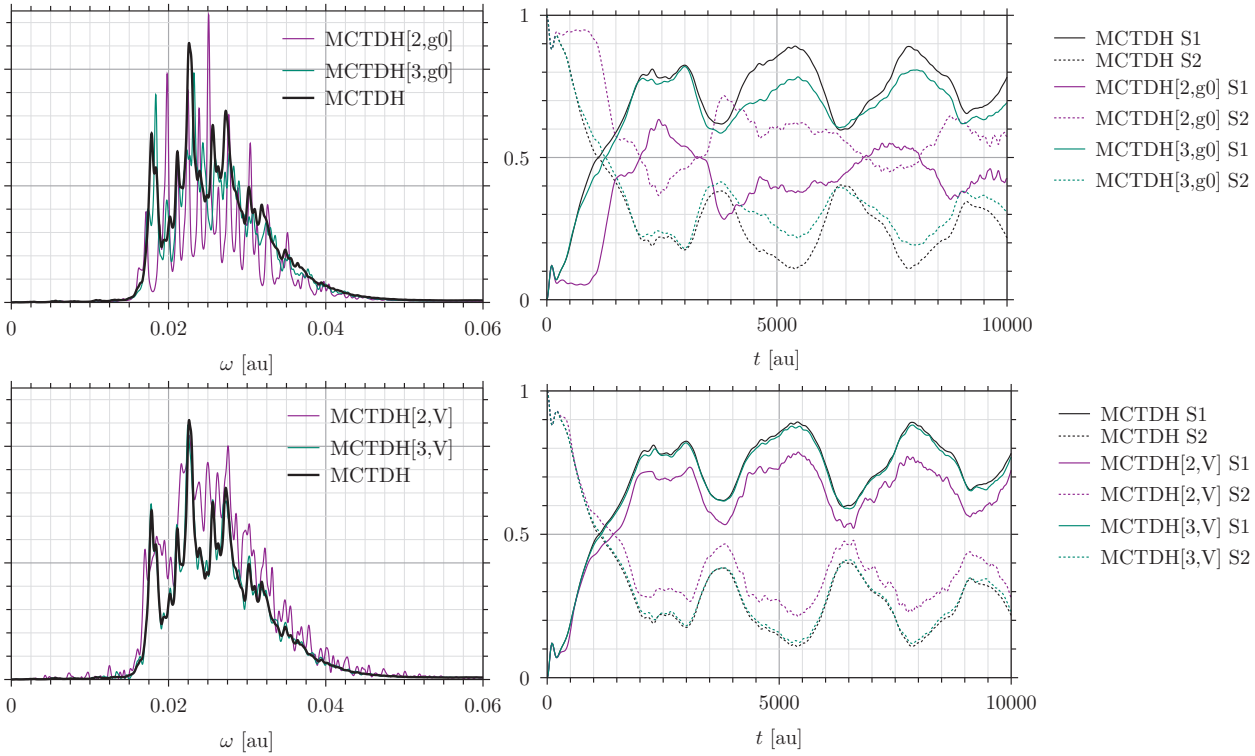

Figure 6: Spectra (left) and diabatic state populations (right) of the 4D pyrazine model using MCTDH[n,g0] and MCTDH[n,V]. A phenomenological broadening of 6200 a.u. $\simeq$ 150 fs is used in the spectra.

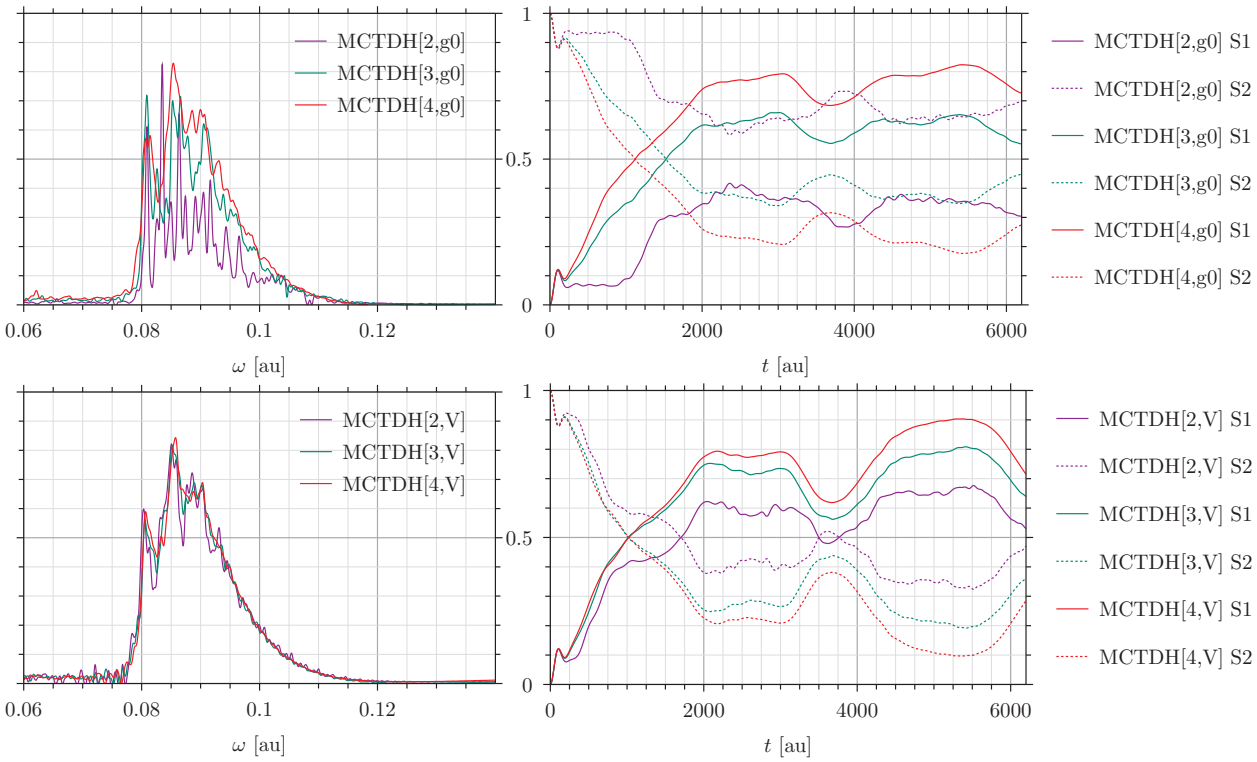

Figure 7: Spectra (left) and diabatic state populations (right) of the 24D pyrazine model using MCTDH[n,g0] and MCTDH[n,V]. A phenomenological broadening of 6200 a.u. $\simeq$ 150 fs is used in the spectra.